Article

Application of Carbide Cutting Inserts as Indenters for Surface Plastic Deformation

Kostiantyn Svirzhevskyi [1], Oleg Zabolotnyi [1,*] , José Machado [2,*] , Anatolii Tkachuk [1] and Inna Boiarska [1]

[1] Applied Mechanics & Mechatronics Department, Lutsk National Technical University, Lvivska Street, 75, 43018 Lutsk, Ukraine

[2] MEtRICs Research Center, University of Minho, Campus of Azurém, 4800-058 Guimarães, Portugal

* Correspondence: volynasi@gmail.com (O.Z.); jmachado@dem.uminho.pt (J.M.)

Abstract: Surface plastic deformation has a high productivity and allows for products with unique operational properties, namely: a high quality of the surface layer, increased support stability of the profile of the treated surface, a strengthened surface layer, and the formation of residual compressive stresses in the surface layer. The essence of smoothing is that a tool with regulated geometric characteristics of the deforming element (indenter) under specific technological processing modes penetrates the surface layer of the workpiece and slides, deforming the microgeometry formed as a result of previous technological operations. The article considers the option of using carbide-cutting plates as deforming elements. For this, a morphological table of methods of spatial orientation of the indenter-plate has been developed, which includes 27 possible options for its installation. The algorithm for calculating the geometry of the contact zone of the indenter and the workpiece is presented. The contact interaction of the indenter plate and the workpiece was studied. On the basis of morphological analysis and conducted applied studies, rational installation angles of the deforming element were determined. The interdependence of the properties of the surface layer on the technological modes of processing was defined.

Keywords: surface plastic deformation; deformation element; carbide cutting plate; geometric characteristics
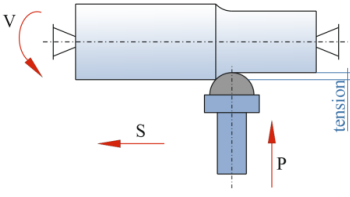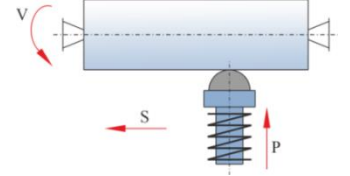
1. Introduction

The technological operation of smoothing is quite well known as one of the methods of surface plastic deformation (SPD). This processing method has wide technological possibilities; with its help it is possible to implement clean finishing, strengthening, and calibration processing [1,2]. The essence of this process is that a tool with certain geometric characteristics of the deforming element (indenter) under regulated technological processing modes penetrates the surface layer of the workpiece and moves, deforming the microgeometry that formed as a result of previous technological operations. As a result of this influence, the physical–mechanical and microgeometrical properties of the surface layer change metal. There are two basic schemes for implementing the SPD process, which are listed in the Table 1 [2,3].

1. Smoothing with a rigid fixation of the tool is implemented with a rigid kinematic connection between the tool and the workpiece. The indenter penetrates the material of the workpiece to a certain depth, which depends on the hardness, plasticity of the material, roughness of the surface layer, and radius of the deforming element. The main technological mode of smoothing with rigid fixation of the tool is the depth of penetration of the indenter into the workpiece material (tension).

2. Smoothing with the elastic fastening of the tool. The tool is pressed against the surface of the workpiece with a regulated force. The magnitude of the force is monitored and maintained by constant monitoring devices during the machining cycle. Structurally, the clamping of the tool is implemented with the help of spring, hydraulic, or pneumatic

systems. The main technological mode during elastic smoothing is the smoothing force (the force pressing the indenter against the surface of the workpiece).

Table 1. Basic schemes of attachment of the tool for processing external surfaces.

№	Processing Scheme	Processing Type	Nomenclature
1		Smoothing with a rigid attachment of the tool	S—longitudinal feed; V—workpiece rotation vector; P—indenter clamping force
2		Smoothing with elastic attachment of the tool	

Schemes for the implementation of smoothing processing methods can be performed in different variations depending on the technological equipment and the shape of the workpiece [3,4]. There is a significant nomenclature of spherical and cylindrical indenters. Spherical indenters are more versatile because they are suitable for processing external and internal surfaces of rotation and flat surfaces. Cylindrical indenters should be used for processing only the external surfaces of rotation. Cylindrical indenters ensure a higher quality of the surface layer and are less prone to the formation of vibrations during processing. Therefore, when processing external cylindrical surfaces, it is advisable to use cylindrical indenters. Considering research regarding the smoothing method using replaceable cutting plates made of various materials as indenters, including ceramics, their use is justified by the results of the system analysis carried out in the paper [5,6].

2. Materials and Methods

The study of the individual characteristics of the smoothing processing methods showed that the static characteristics remained the least studied, namely, the method of installing the indenter, the basis of which further development of the surface plastic deformation method is possible. Figure 1 shows a scheme for processing external cylindrical surfaces of rotation using a cylindrical indenter at angle α.
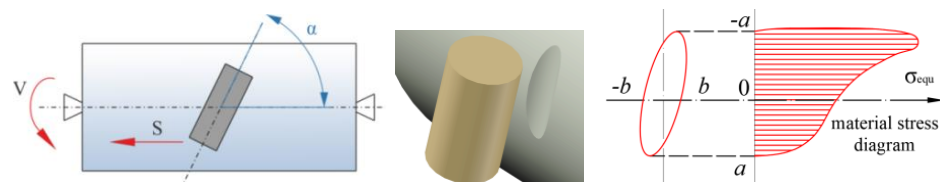
Figure 1. The scheme of processing by smoothing with the installation of an indenter at angle α. α—the angle of rotation of the indenter in the axial direction; a, $-a$ are the axes of the major focus of the ellipse; b, $-b$ are the axes of the minor focus of the ellipse; σ_{egu}—residual compressive stresses.

During processing with a cylindrical indenter, the tool was installed perpendicular to the axis of rotation of the workpiece or at a certain angle to the side opposite the feed direction. Smoothing with the installation of the indenter at an angle was similar to smoothing without turning the indenter, but with an increased radius. A group of static characteristics allowed for the use of different indenter shapes, so it became possible to transform the cutting process into SPD quite easily, and by changing the method of installing the cutting plate, it combined the cutting and SPD processes [7,8]. In Figure 2

shows a diagram of the installation of the tool with interchangeable plates, which allows for performing smoothing processing. The method of installation of the replaceable plate had an impact on the technological capabilities of the smoothing process and the quality parameters of the part [9,10].
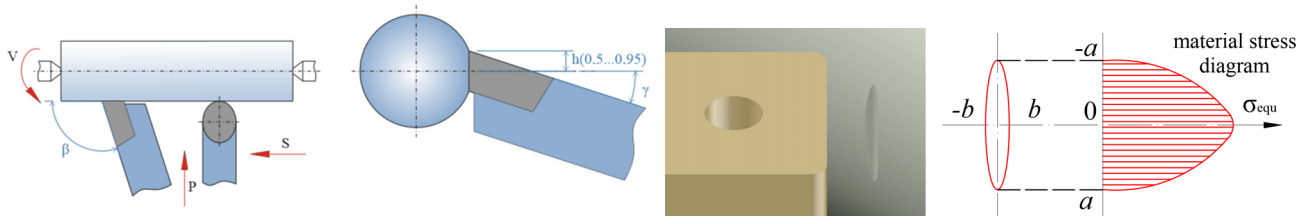

Figure 2. Scheme of smoothing processing using a carbide cutting plate as an indenter β—the angle of installation of the tool in the axial direction; γ—tool setting angle in the radial direction; h (0.5 . . . 0.95)—displacement of the cutting edge of the tool relative to the center of the workpiece.

Changing the way the plates were installed was equivalent to changing their geometry, which allowed for using its different sections to implement the processing process. A morphological analysis of the indenter installation schemes was performed to identify a variety of tool installation options [11]. Morphological synthesis of methods of installing the indenter, in the form of a variable plate, made it possible to obtain a morphological table of methods of spatial orientation of the indenter plate (Figure 3), which included 27 possible variants of its orientation. Each installation option was considered in a three-coordinate scheme, in which each position of the tool was provided by the corresponding angles of rotation by a certain amount around one, two, or three axes, separately or simultaneously [12,13]. The value of the angle of rotation of the plate was determined in such a way that the stable quality of the surface layer was ensured in the stationary processing mode.
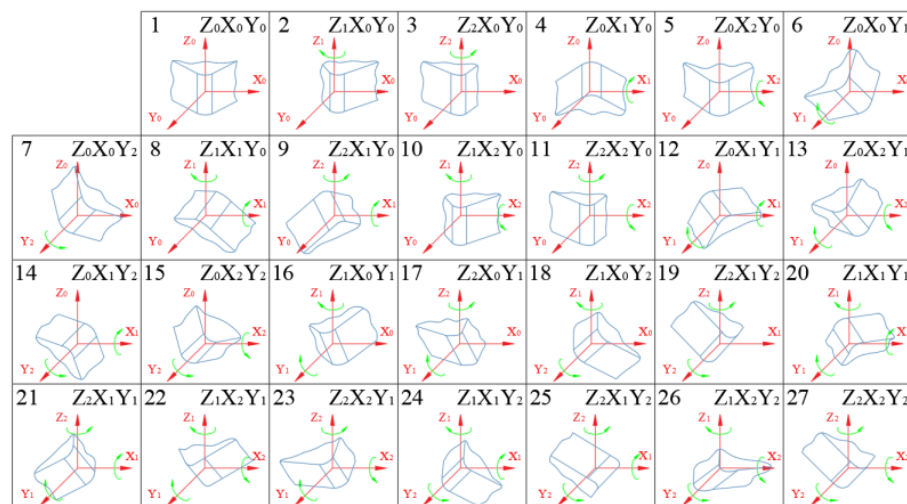

Figure 3. Morphological table of possible options for installing the indenter plate.

The direction of the rotation angle of the indenter plate was determined as conditionally negative and conditionally positive, which is evidenced by the indices 0, 1, and 2 next to the designation of the coordinate axes. The index "0" indicated that the tool had no rotation angle around this axis. Index "1" was set in the case when the rotation of the indenter plate around the axis occurred in a conditionally positive direction, which coincided with the clockwise movement. Index "2" indicated that the rotation of the indenter plate was made by a negative angle (counter clockwise). The result of the morphological analysis was the determination of the spatial orientation of the indenter plate depending on the method of installation of the tool:

(1) installation methods according to schemes 1 ... 4, 6 ... 9, 12, 14, 16 ... 21, and 25 provided smoothing of the external cylindrical surfaces;

(2) installation methods 22, 23, 24, and 27 provided combined processing by cutting and SPD;

(3) installation methods 5, 10, 11, 13, 15, and 26 provided standard turning processing.

Installation of the indenter plate according to scheme 22 allowed for cutting of the pre-strengthened layer, which led to a decrease in the cutting force and uniformity of the cut layer; when installing according to method 24, the allowance for mechanical processing was first cut and then smoothed, which ensured an increase in the quality of the processed surface. The installation of the tool according to schemes 23 and 27 provided smoothing and turning processing at the same time. In scheme 23, the main part belonged to smoothing, and only some work for forming the surface was done by the method of fine-tuning, and in scheme 27, the main processing was carried out by cutting, and smoothing took place only with some smoothing of the microgeometry. Installation of the tool according to scheme 5, but with an upward shift along the OZ axis, would provide combined cutting (cutting edge) processing with subsequent smoothing (the back surface and the radius of the transition surfaces of the indenter plate). Changing the way the tool was installed provided a different geometry for the contact zone of the indenter plate with the surface of the workpiece. This, in turn, significantly affected such parameters of the smoothing process, such as the average pressure in the contact spot, smoothing force, cyclic load, friction conditions, and temperature, which formed the quality parameters of the surface layer of the part [14,15].

The size of the contact patch is usually determined by the two characteristics in Table 2:

Table 2. Expressions for determining the geometric parameters of the contact zone.

№	An Expression for Determining the Parameters of the Contact Zone	Author
1	$a \cong \sqrt{2R_p(h+\Delta)}; \qquad -a \cong \sqrt{2R_p\Delta};$ $b \cong \sqrt{\frac{2R_iR_p}{R_i+R_p}(h+\Delta)}; \qquad -b \cong \sqrt{\frac{2R_iR_p}{R_i+R_p}\Delta};$ R_i, R_p—the radius of the indenter and the part, respectively; h—residual deformation; Δ—elastic deformation	[3]
2	$a = \sqrt{2R(h_h+h_e+h_p)}; \quad -a = \sqrt{2R\left(h_h+\frac{1}{3}h_e\right)};$ $b = \sqrt{2a_1(S-S^2)}; \qquad -b = 0.8\sqrt{Rh_p};$ R—indenter radius; h_e, h_p—depth of elastic and plastic penetration of the indenter; h_h—wave height in front of the indenter; S—feed	[3]
3	$a = \frac{\sin\varphi_S}{\rho_S}; \quad b = \frac{\sin\varphi_V}{\rho_V}$ $\sin\varphi_S$, $\sin\varphi_V$—the sines of the angles of penetration of the feed plane and the velocity vector, respectively; ρ_S, ρ_V—the curvature of the tangent elements in the plane that passes through the axis of the workpiece in the plane of the velocity vector	[5]
4	$b = a\sqrt{\frac{R_W}{R_{DE}}} \cdot \frac{2\cos\psi}{1+\sqrt{1-\left(\frac{a\cos\psi}{R_{DE}}\right)^2}}$ R_W—workpiece radius; R_{DE}—the radius of the deforming element; ψ—rotation angle relative to the horizontal axis (parallel to the feed vector)	[3]

(1) the contact width is the distance between the initial and final points of contact of the indenter with the processed surface in the direction of the feed movement;

(2) contact length—the distance between the initial and final points of contact of the deforming element with the surface of the workpiece in the direction of the speed vector of the main processing movement.

The width and length of the contact patch were formed in two areas: the first (the most loaded area) ensured plastic interaction of the front surface of the deforming element with the surface of the workpiece; the second area provided elastic interaction on the rear surface of the deformable element. The contact area was the main parameter that determined the amount of contact pressure, intensity of deformation, cyclic load, process productivity, and thermal tension of the contact interaction of the tool with the workpiece [16,17]. The actual contact area always differed from the calculated one due to the roughness and waviness of actual surfaces [18,19]. Table 3 presents analytical dependencies for calculating the contact area, for different processing conditions and shapes of the working part of the deforming element during SPD.

Table 3. Analytical expressions for determining the contact area during smoothing.

Indenter Form	An Expression to Define A Parameter	Author
Sphere	$F = \frac{\pi}{2} R R z$; $F = \pi \frac{\sin \varphi_S \sin \varphi_V}{\rho_S \rho_V}$	
Conical roller	$F = \frac{\pi \sin \varphi_S \sin \varphi_V}{2 \rho_S \rho_V} \left(1 + \frac{\sin \varphi_1}{2 tg \xi}\right)$	
Thoroconus	$F = \frac{\pi}{2} \rho_S^{-1.5} \rho_V^{-0.5} (2 \sin \varphi - tg \xi)^2 \left(\frac{1 + 2 \sin \varphi - tg \xi}{2 tg \xi} \sqrt{\frac{\rho_S}{\rho_V}}\right)$	
Spherocone	$F = \frac{\pi}{2} \left(\frac{R}{\cos \gamma}\right)^2 (2 \sin \varphi - tg \xi)^2 \left(1 + \frac{2 \sin \varphi - tg \xi}{2 tg \xi \sqrt{\cos \gamma}}\right)$	[3]
Cylinder with installation at an angle	$F = 4\pi \sin^2 \varphi \left[\left(1 + \sqrt{\frac{\rho_a}{\rho_b}}\right)\left(1 + \sqrt{\frac{\rho_b}{\rho_a}}\right)\rho_a \rho_b\right]^{-1}$; $\rho_a = \frac{\sin^2 \gamma}{R_3}$; $\rho_b = \frac{\cos^2 \gamma}{R_w} + \frac{1}{R}$ ρ_S, ρ_V—curvature of the tangential elements in the plane of supply and the plane of the velocity vector; $\sin \varphi_S$, $\sin \varphi_V$—the sines of the penetration angles in the feed plane and the velocity vector; φ—penetration angle; ξ—the angle between the source of the indenter and the workpiece; φ_1, φ_2—penetration angles of the torus part of the roller; ρ_a, ρ_b—contact curvature in the plane that passes through the axis of the cylinder and the workpiece; γ—angle of inclination of the axis of the indenter cylinder to the axis of the workpiece; R_w, R—workpiece and indenter radius	

To solve this problem, an algorithm for calculating the geometry of the contact area was developed (Figure 4) and a mathematical model based on this algorithm was created. Output data of the algorithm: r—radius of the variable plate (mm); R_0—workpiece radius (mm); i—technological tension (μm); φ', ψ—the radius of the turning angle of the tool (degrees); a—the length of the major semi-axis of the ellipse (determined experimentally) (mm); K_M—coefficient that takes into account the material of the part.

It was not convenient to perform calculations in this way, because the analytical expressions were quite complex. In addition, among the initial data was the value a, which was determined experimentally (the length of the contact area of the tool with the workpiece). The disadvantages of this model are also that the depth of penetration of the indenter plate into the material of the workpiece was not taken into account in the calculations, and the physical and mechanical properties of the material were taken into account indirectly—with the help of the K_M coefficient.

To determine the depth of penetration of the indenter-plate into the metal of the workpiece h and the interdependencies of its change when changing the tool installation method, a number of experiments were conducted in which the smoothing process was interrupted in the constant processing mode. As a result, profilograms of the transition area between the processed and untreated surfaces of the workpiece were obtained. The recording of profilograms of the transition zone was carried out on a Mahr MarSarf M300

profilograph profilometer. During the analysis of profilograms, the depth h was established. C45 steel shafts with a diameter of 70 to 85 mm were used as samples.
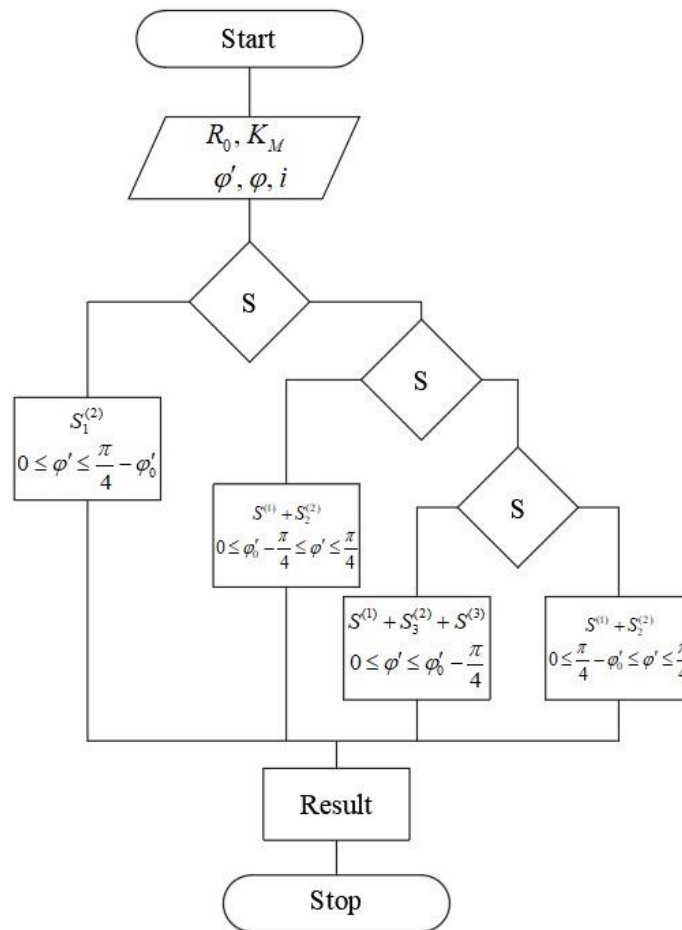

Figure 4. The algorithm for calculating the contact geometry of the indenter and the workpiece.

3. Results

Schemes from the morphological table of possible ways of installing indenter plates (Figure 3) that provide smoothing processing were studied: scheme no. 1, where the indenter plate was in the initial position, $\varphi' = \psi = 0°$; schemes no. 2, 3, 6, and 7, where the indenter plate rotates around one of the axes; schemes no. 16, 17, 18, and 19, where the indenter plate rotates around the two axes, OZ and OY, at the same time by the angles $\pm\varphi'$ and $\pm\psi$, respectively. More than 50 profilograms of the transition zone between the treated and untreated surfaces were analyzed. This made it possible to establish that the depth of penetration h and the width of the contact area α (as a result, the contact area) depended on the tool installation scheme. The rotation of the indenter plate by an angle φ' around the vertical axis OZ in the intervals $[-10°; 0°]$ and $[0°; 10°]$ significantly increased (by 2 ... 3 times) the depth of penetration of the deforming element, due to the redistribution of forces that arose in the process of smoothing (Figure 5). When turning to an angle $-\varphi'$ (in the direction of movement of the tool's longitudinal feed), the depth of penetration of the deforming element increased by $10-15\%$ more than when turning in the positive direction. An increase in the depth of penetration led to a proportional increase in area F and the width of contact a. The shape of the contact patch remained practically unchanged. When the indenter plate was rotated by angle φ', it was an elliptical impression with the major semi-axis oriented along the speed vector of the main smoothing movement.
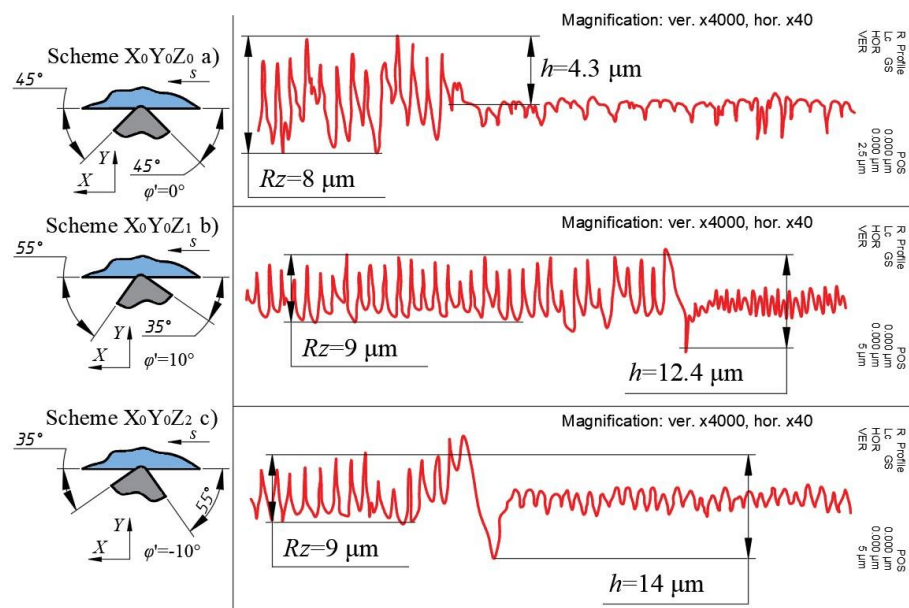
Figure 5. Profilograms of deformation centers during the rotation of the indenter plate around the vertical axis OZ.

The angle of rotation of the indenter plate around the horizontal axis OY did not lead to a significant change in the depth of penetration h, as the installation of the tool at an angle ψ actually increased the radius of the indenter plate in the plane parallel to the feed movement. An increase in the radius of the tool entailed an increase in the contact area and thus a decrease in the depth of penetration, as more effort was required to ensure sufficient specific pressure of the penetration of the tool into the material. Because of the rotation of the elliptical contact spot in the direction of the axis of the workpiece, the width of the contact increased without a noticeable increase in the area of the contact spot F (Figure 6).
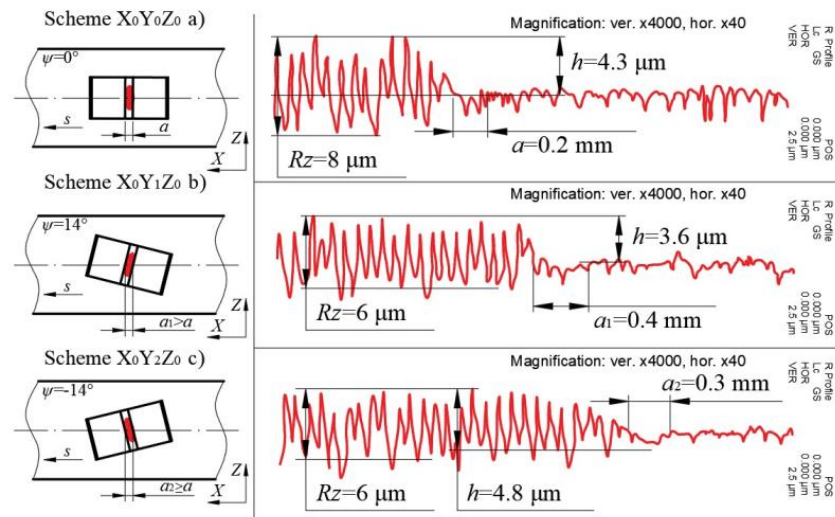

Figure 6. Profilograms of deformation centers during rotation of the indenter plate around the horizontal axis OY.

Dependences of the relative penetration of the tool into the material of the workpiece on the installation angles of the indenter plates were obtained using regression analysis of graphical dependencies constructed from experimental data (Figure 7). The degree of accuracy of the regression equation was up to 15%.
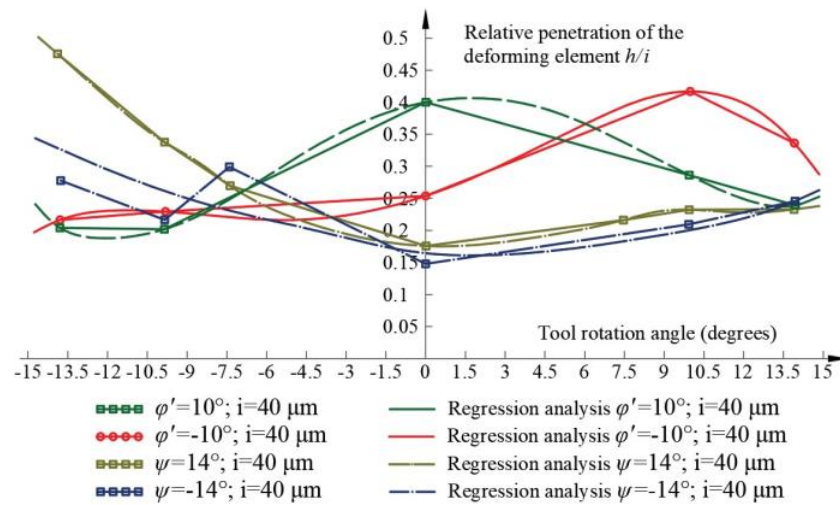
Figure 7. Dependence of the value of the relative penetration on the method of installation of the indenter plate.

The relative penetration was defined as the ratio of the value of the depth of penetration h to the technological tension i. It can be seen from the graphs that the greatest relative penetration of the deforming element was achieved when the tool was installed according to schemes no. 2 and no. 17. The smallest relative penetration was observed when the deforming element was installed according to schemes no. 6 and no. 7. The range of plate rotation angles was set experimentally in the range from $-15°$ to $15°$, when the indenter plates were installed at large rotation angles, the penetration depth h, and thus the relative penetration h/i decreased sharply. The reason is that as the width of the contact increased, the area also increased, and as the angle of rotation φ' increased, conditions arose that facilitated the penetration of the deforming element into the material of the workpiece, as a result of which the necessary smoothing force increased proportionally. This led to an increase in elastic impressions in the technological system.

In order to determine the penetration depth h, which was necessary to determine the plastic contact area, graphical dependencies were constructed based on experimental data and their regression analysis was performed. As a result, approximation curves were obtained (Figure 8), with the help of which it was possible to determine the depth of penetration, which corresponded to one or another scheme of installation of indenter plates (determined by the angles φ' and ψ). The degree of accuracy of the regression equation was up to 15%.
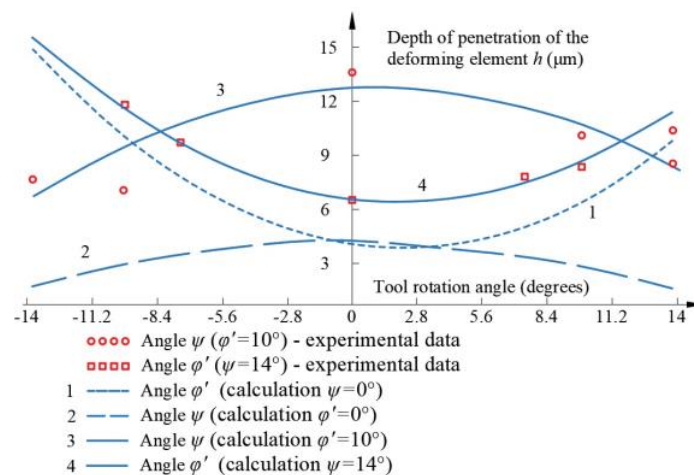

Figure 8. Dependence of the penetration depth of the deforming element h on the tool installation angles.

The analytical expression for determining the penetration depth of the tool based on the specified values (and directions) of the rotation angles φ' and ψ was found from the graphical solution of the system of equations with two unknowns. Approximation curves for the dependence of h on each of the two angles separately were used as equations:

$$h = 0.043277\varphi'^2 - 0.18758\varphi' - 0.013\psi^2 - 0.0078\psi + 3.35. \tag{1}$$

Expression (1) allows for calculating the depth of penetration of the deforming element h with a sufficient degree of accuracy, within 15%, without conducting complex experiments to obtain the center of deformation and to study its profilograms.

3.1. Determination of the Area and Width of the Contact Zone

After determining the penetration depth h of the deforming element into the workpiece material, according to the installation diagrams, the values of the areas of plastic contact F_Π were calculated, and the smoothing force P [20,21] was calculated:

$$P = F_\Pi \cdot HV. \tag{2}$$

Having determined the level of the smoothing force corresponding to the tool installation diagrams, it was possible to calculate the full contact area of the indenter plate with the workpiece F. Formula (3) was used to calculate the full contact area, the average pressure in the contact zone, and the cycle of the load.

$$F = Fn + Fy = 0.75\left[\frac{P}{HV} + 2.32\left(\frac{1-\mu}{E}R' \cdot P\right)^{\frac{2}{3}}\right] \tag{3}$$

After the calculations, construction of the graphical dependencies, and regression analysis, analytical and graphical dependences of the full contact area of the deforming element and the surface of the workpiece on the method of tool installation were obtained (Figure 9). The analytical expression for determining the full contact area F, the analyzed indenter plate installation scheme, was obtained using regression analysis of the experimental data:

$$F = 0.00187\varphi'^2 - 0.00746\varphi' + 0.00074\psi^2 + 0.00148\psi + 0.179. \tag{4}$$
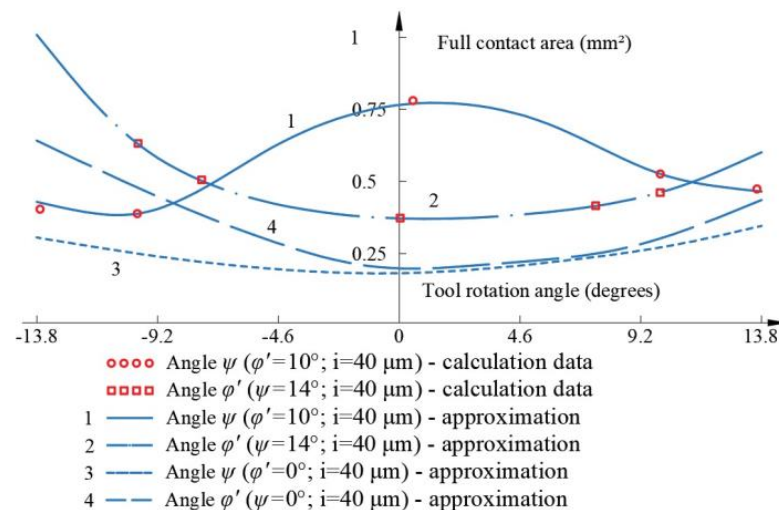

Figure 9. Dependence of the total contact area F on the method of tool installation.

As can be seen from the graph in Figure 9, the total contact area varied when changing the magnitude and direction of the rotation angles of the indenter plates. The nature of the dependences had a lot in common with the dependence of the penetration depth h on the method of installing the deforming element (Figure 8). This is explained by the fact that the contact area F and the width of the contact spot were largely determined by the penetration depth h of the indenter plate into the workpiece material.

The angle of rotation of the plate φ' led to an increase in the total contact area regardless of the direction of its rotation. When turning to an angle $-\varphi'$, the contact area increased more intensively, because the actual penetration of the indenter plate was greater when the plate was turned in the direction of the tool feed movement, with other technological parameters remaining constant. When installing plates with rotation angles φ' that exceeded the interval $[-14°; 14°]$, it wsa necessary to reduce the technological tension, as an increase in the contact area by more than $0.8 \ldots 0.9$ mm led to a significant increase in force, which could cause the destruction of the surface layer of the workpiece or disrupt the stability of the processing process and lead to strong vibrations. Using the scheme with the elastic fastening of the tool for assigning angles φ' outside the range of values $[-14°; 14°]$ required the appointment of a large smoothing force, which could also degrade the quality of the machining process. Therefore, the use of schemes for installing indenter plates with rotation angles φ' greater than $14°$ was advisable for strengthening processing on machines with high rigidity and high-quality feed systems.

A decrease in the contact area F was not accompanied by a pronounced decrease in the width of the contact spot a, which contributed to the preservation of the cyclic load, which corresponded to contact with a larger area. This feature of the installation scheme of deforming elements with a corner turn could be used for fine finishing with minimal smoothing efforts. When the rotation angles of the indenter plates φ' and ψ increased in both directions, the width of the contact spot was increased (Figure 10). In the first case, this was due to an increase in the contact width due to an increase in the penetration depth h, and in the second case, due to an increase in the contact width when the elliptical contact area was rotated along the axis of rotation of the workpiece.
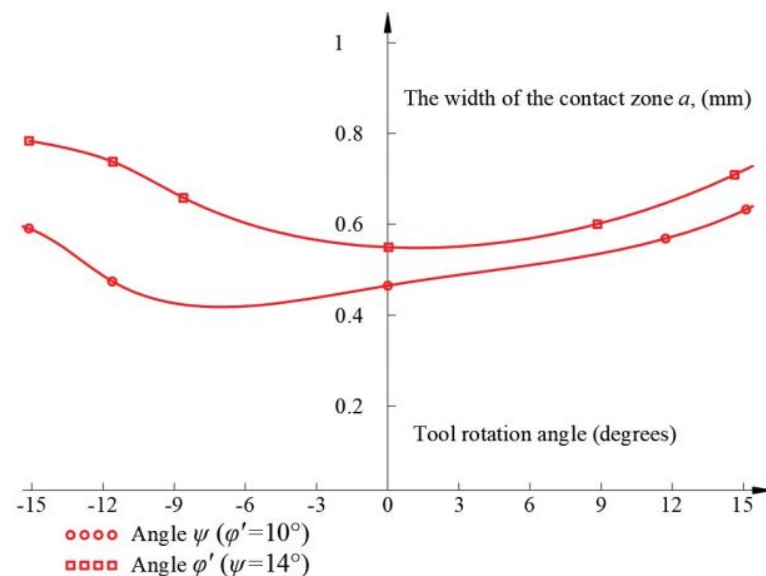

Figure 10. Dependence of the width of the contact patch, a, on the method of installing the tool.

To check the adequacy of the methodology for calculating the full area F and width a of the contact spot, the following experiments were conducted: smoothing processing was performed with indenter plates with a CVD coating, on which a trace remained after one pass, the resulting area was determined on a contact-optical coordinate measuring machine DKM 1-300DP. The measurement results showed a discrepancy with the calculated data within 10%.

3.2. Determination of the Smoothing Force, the Average Pressure in the Contact Zone, and Cyclic Loading

The smoothing force P was calculated according to Formula (2), and the average contact pressure was calculated as follows:

$$p = P/F, \tag{5}$$

where F is the total contact area (mm^2) and P is the smoothing force (N).

When changing the method of installing the deforming element, the smoothing force varied in a wide range (Figures 11 and 12). The force reached the highest values (1200 . . . 1400 N) when the indenter-plate was installed with a rotation around the vertical axis at an angle of $-\varphi' = -7° \ldots -14°$; at the same time, it increased directly proportionally and the contact area was thus the average of the pressure in the contact zone p, which increased less intensively from 1500 to 1800 (MPa) (Figure 11).
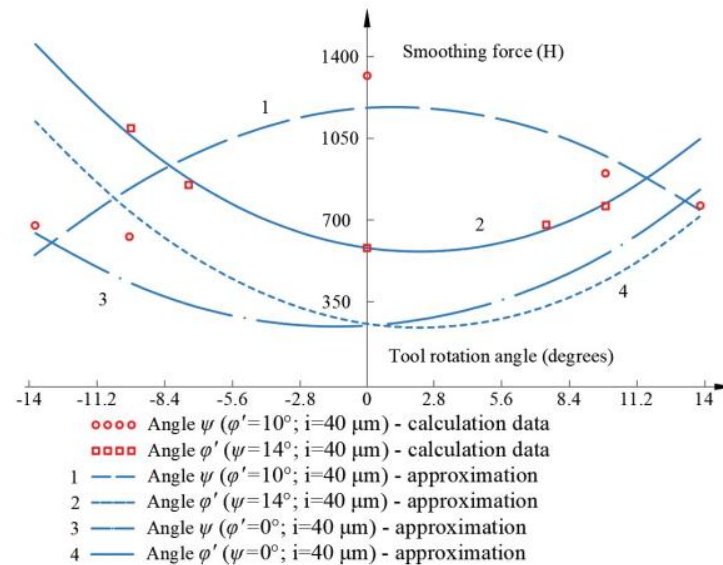
Figure 11. Dependence of the smoothing force P on the installation angles of the deforming element.
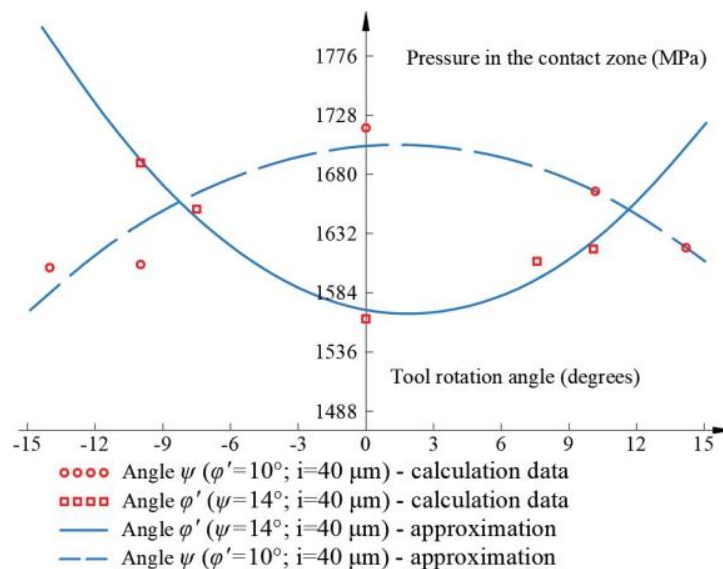
Figure 12. Dependence of the average pressure in the contact zone p on the installation angles of the deforming element.

The dependence of the smoothing force on the magnitude and direction of the angle of rotation ψ (around the horizontal axis OY) had a different character—when the angle of rotation ψ increased, the force increased less intensively (compared with the rotation by the angle φ'), approximately by a factor of 2 at intervals of changing angle ψ $[-14°; 0°]$ and $[0°; 14°]$. When turning the indenter plate to angles φ' and ψ simultaneously, the

smoothing force decreased (approximately from 1100 to 500 N at $\varphi' = 10°$), but due to a proportional decrease in the contact area, the pressure also changed (1600 . . . 1700 MPa).

To assess the degree of adequacy of the developed method for calculating the processing force, an experiment was conducted to measure the smoothing force using a universal dynamometer UDM-600. A C45 steel sample with an initial roughness of Ra = 2.5 (µm) was machined with an indenter plate according to the $X_0Y_0Z_0$ scheme (installation angles $\varphi' = \psi = 0°$), with a given technological tension i = 10 (µm), at a speed of V = 100 (m/min) and feed s = 0.l (mm/rev). Differences between experimental data and calculated values were within 15%.

When using an indenter plate as a tool, the power parameters of the smoothing process approach, in terms of their values, are the force and the pressure that occurs during power smoothing processing or rolling with rollers. The large values for the smoothing force and the average pressure in the contact zone were explained by the fact that the contact area of the deforming element with the workpiece was significantly larger (2 . . . 4 times) than the contact area of a standard spherical indenter. This made it possible to apply smoothing with indenter plates during high-speed processing of surfaces of rotation with feeds (up to s = 0.12 . . . 0.15 mm/rev). The cyclic load N was calculated according to the formula:

$$N = a/s, \tag{6}$$

where a is the width of the contact spot (mm) and s is the movement of the tool feed (mm/rev).

The magnitude of cyclic loading (for feed s = 0.08 mm/rev) increased in the interval 4 to 10 times when rotating the deforming element around the vertical axis OZ by the angle φ' in the intervals $[-10°; 0°]$ and $[0°; 10°]$ and around the horizontal axis OY by the angle ψ in the intervals $[-14°; 0°]$ and $[0°; 14°]$, respectively (Figure 13).
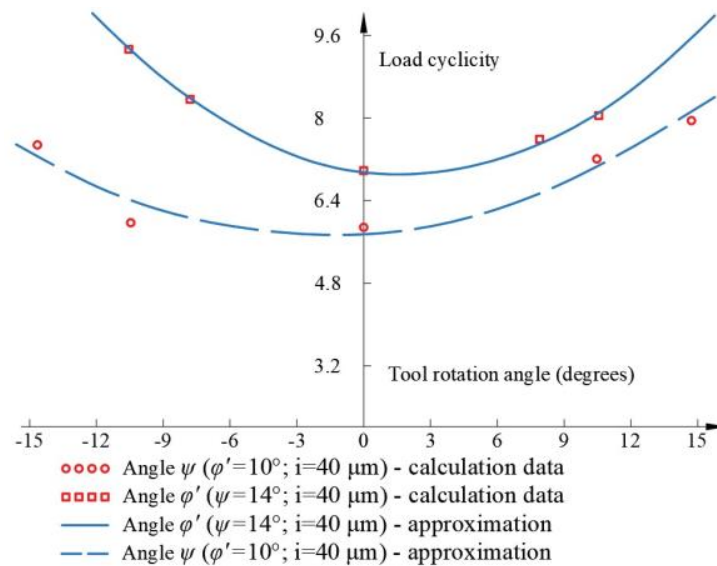

Figure 13. Dependence of cyclic load N on the installation angles of the indenter plate.

In the first case, this was due to an increase in the width of the contact due to an increase in the depth of penetration, and in the second, due to an increase in the width of the contact spot when the indenter plate was rotated along the axis of rotation of the workpiece. An increase in the load cyclicity N together with an increase in the rotation angles of the deforming element means that there was an opportunity to assign a large tool feed, remaining in the load cyclic interval, for strengthening and smoothing processing ($6 \leq N \leq 20$), which led to an increase in the productivity of the smoothing process while maintaining the regulated quality of the surface layer of the workpiece.

4. Conclusions

The article proved that not only special indenters, but also standard plates for turning, could be used as a deforming element for smoothing processing, changing the way they were installed. Based on the analysis of possible methods of installing indenter plates for smoothing the external surfaces of rotation, it was established that the method of installing the plates significantly affected the technological possibilities of the smoothing process and the quality parameters of the treated surfaces. When changing the tool installation scheme, the geometric parameters of the contact area (area and dimensions of the contact spot) of the indenter plate with the workpiece also changed.

1. The installation angles of the indenter plate φ' and ψ, depending on their magnitude and direction of rotation, affected the penetration depth h of the deforming element during smoothing with the tool fixed according to a rigid scheme. In the case of installing an indenter plate with a rotation angle φ' from $0°$ to $\pm 14°$, the penetration depth h increased by 2 to 3 times.
2. Installation of the tool with rotation angles φ' exceeding $[-14°; 14°]$ increased the size of the contact area to $0.8 \ldots 0.9$ mm^2 and more, leading to a significant increase in the smoothing force. Which reduced the quality of the treated surface.
3. As the angles of rotation of the tool φ' and ψ increased in both directions, the width of the contact spot increased. In the first case, this was due to an increase in the contact width due to an increase in the penetration depth h, and in the second, due to an increase in the contact width when the plate rotated around the horizontal axis OY and the elongation of the semi-axes of the elliptical contact zone.
4. The smoothing force reached the highest values in the case of installing the plate with a rotation around the vertical axis at an angle $\varphi' = -14° \ldots -10°$; $1000 \ldots 1400$ (N). The contact area also increased in direct proportion—therefore, the average pressure in the contact p increased less intensively from 1500 to 1800 (MPa). As the angle of rotation ψ increased, the smoothing force increased, approximately by a factor of 2 in the intervals of change of angle ψ $[-14°; 0°]$ and $[0°; 14°]$.
5. When turning the tool to angles φ' and ψ (at the same time, the smoothing force decreases (from approximately 1100 to 500 (N) at $\varphi' = 10°$), but due to a proportional decrease in the contact area, the pressure remained practically unchanged (1600 to 1700 MPa).
6. In the case of use as a tool for smoothing indenter plates, the power parameters of the processing process approach, there is consideration of their dimensions, force, and pressure that occurs during processing by power diamond smoothing or rolling. This makes it possible to use smoothing with indenter plates for the rapid processing of rotational surfaces with a feed rate (of up to 0.16 mm/rev).

A further prospect of research may be a combined technology that will combine the technological operation of cutting and plastic deformation. The parts processed by this technology will have regulated parameters of microgeometry and unique physical and mechanical properties.

Author Contributions: Conceptualization, K.S., O.Z. and J.M.; methodology, O.Z.; software, K.S. and A.T.; validation, O.Z., J.M. and I.B.; formal analysis, O.Z.; investigation, K.S., A.T. and I.B.; resources, O.Z., J.M.; data curation, O.Z.; writing—original draft preparation, K.S., A.T., I.B.; writing—review and editing, O.Z. and J.M.; visualization, K.S., O.Z., J.M., A.T. and I.B.; supervision, O.Z. and J.M; project administration, O.Z. and J.M.; funding acquisition, O.Z. and J.M. All authors have read and agreed to the published version of the manuscript.

Institutional Review Board Statement: Not applicable.

Informed Consent Statement: Not applicable.

Conflicts of Interest: The authors declare no conflict of interest.

References

1. Deng, L.; Luo, B.; Cheng, H.; Lin, W.; Cheng, L.; Wang, Q. Effect of yield hardening on plastic deformation of metal contact interface. In Proceedings of the 2021 3rd International Academic Exchange Conference on Science and Technology Innovation (IAECST), Guangzhou, China, 10–12 December 2021; pp. 1975–1980. [CrossRef]
2. Cai, W.; Zhang, Y.; Li, L.; Peng, T.; Lai, K.H.; Wiercigroch, M. Cutting mechanics and efficiency of forward and reverse multidirectional turning. *Int. J. Mech. Sci.* **2023**, *242*, 108031. [CrossRef]
3. Zablotskyi, V.; Moroz, S.; Tkachuk, A.; Prystupa, S.; Zabolotnyi, O. Influence of Diamond Smoothering Treatment Power Parameters on Microgeometry of Working Surfaces of Conjugated Parts. In *Advanced Manufacturing Processes. InterPartner 2019*; Lecture Notes in Mechanical Engineering; Springer: Cham, Switzerland, 2020; pp. 370–377. [CrossRef]
4. Falta, J.; Sulitka, M.; Janota, M.; Frkal, V. Model of force interaction for stability prediction in turning of thin-walled cylindrical workpiece. *Int. J. Adv. Manuf. Technol.* **2023**, *125*, 195–212. [CrossRef]
5. Stelmakh, A.; Kostunik, R.; Radzievskyi, V.; Shymchuk, S.; Zaichuk, N. An Increase in Tribocharacteristics for Highly Loaded Friction Units of Modern Equipment. In *Advances in Design, Simulation and Manufacturing V. DSMIE 2022*; Ivanov, V., Trojanowska, J., Pavlenko, I., Rauch, E., Peraković, D., Eds.; Lecture Notes in Mechanical Engineering; Springer: Cham, Switzerland, 2022; pp. 504–518. [CrossRef]
6. Sharma, R.; Pradhan, S.; Bathe, R.N. Comparison, validation, and prediction of machinability aspects of textured and non-textured cutting inserts. *J. Braz. Soc. Mech. Sci. Eng.* **2023**, *45*, 76. [CrossRef]
7. Ivanov, V.; Dehtiarov, I.; Pavlenko, I.; Kosov, I.; Kosov, M. Technology for complex parts machining in multiproduct manufacturing. *Manag. Prod. Eng. Rev.* **2019**, *10*, 25–36.
8. Mikołajczyk, T.; Latos, H.; Szczepaniak, Z.; Paczkowski, T.; Pimenov, D.Y.; Giasin, K.; Kuntoğlu, M. Theoretical and experimental research of edge inclination angle effect on minimum uncut chip thickness in oblique cutting of C45 steel. *Int. J. Adv. Manuf. Technol.* **2023**, *124*, 2299–2312. [CrossRef]
9. Svirzhevskyi, K.; Zabolotnyi, O.; Tkachuk, A.; Machado, J.; Kononenko, A. An Increase in Wear Resistance Frictional Contact of Functional Surfaces for Plunger Pairs. In *Advances in Design, Simulation and Manufacturing IV. DSMIE 2021*; Ivanov, V., Pavlenko, I., Liaposhchenko, O., Machado, J., Edl, M., Eds.; Lecture Notes in Mechanical Engineering; Springer: Cham, Switzerland, 2021; pp. 84–94. [CrossRef]
10. Joyson Selvakumar, S.; Sakthivel, P.; Praveen, J.A.; Samuel Raj, D. Effect of edge radius on forces, tool wear and surface integrity under edge radius dominated tool-chip contact conditions. *Proc. Inst. Mech. Eng. Part B J. Eng. Manuf.* **2023**. [CrossRef]
11. Svirzhevskyi, K.; Zabolotnyi, O.; Tkachuk, A.; Zablotskyi, V.; Cagáňová, D. Methods of Evaluating the Wear Resistance of the Contact Surfaces of Rolling Bearings. In *Advanced Manufacturing Processes II. InterPartner 2020*; Tonkonogyi, V., Ivanov, V., Trojanowska, J., Oborskyi, G., Grabchenko, A., Pavlenko, I., Edl, M., Kuric, I., Dasic, P., Eds.; Lecture Notes in Mechanical Engineering; Springer: Cham, Switzerland, 2021; pp. 453–463. [CrossRef]
12. Denkena, B.; Abrão, A.; Krödel, A.; Meyer, K. Analytic roughness prediction by deep rolling. *Prod. Eng.* **2020**, *14*, 345–354. [CrossRef]
13. Imbirovych, N.; Povstyanoy, O.; Zaleta, O.; Shymchuk, S.; Priadko, O. The Influence of Synthesis Modes on Operational Properties of Oxide Ceramic Coatings on Aluminum Alloys. In *Advances in Design, Simulation and Manufacturing IV. DSMIE 2021*; Ivanov, V., Trojanowska, J., Pavlenko, I., Zajac, J., Peraković, D., Eds.; Lecture Notes in Mechanical Engineering; Springer: Cham, Switzerland, 2021; pp. 536–545. [CrossRef]
14. Maximov, J.T.; Duncheva, G.V.; Anchev, A.P.; Dunchev, V.P. Slide burnishing versus deep rolling—A comparative analysis. *Int. J. Adv. Manuf. Technol.* **2020**, *110*, 1923–1939. [CrossRef]
15. Jozwik, J.; Pytka, J.; Legutko, S.; Tofil, A. Surface Morphology Analysis After Sintered Carbon Milling Process. In Proceedings of the 2019 IEEE 5th International Workshop on Metrology for AeroSpace (MetroAeroSpace), Turin, Italy, 19–21 June 2019; pp. 381–386. [CrossRef]
16. Babak, V.; Bilchuk, Y.; Shchepetov, V. Increased wear coatings due intrastructural selfcorrection. *J. Eng. Sci.* **2019**, *6*, 11–15.
17. Dzyura, V.; Maruschak, P. Optimizing the Formation of Hydraulic Cylinder Surfaces, Taking into Account Their Microrelief Topography Analyzed during Different Operations. *Machines* **2021**, *9*, 116. [CrossRef]
18. Yaroshevich, N.; Zabrodets, I.; Shymchuk, S.; Yaroshevich, T. Influence of elasticity of unbalance drive in vibration machines on its oscillations. *East.-Eur. J. Enterp. Technol.* **2018**, *5*, 62–69. [CrossRef]
19. Lu, X.; Jia, Z.; Jia, D.; Yang, J. Smoothing treatment and tool compensation of surface scan tracking measurement sampling data. In Proceedings of the 2009 9th International Conference on Electronic Measurement & Instruments, Beijing, China, 16–19 August 2009; pp. 1-177–1-181. [CrossRef]

20. Schubnell, J.; Farajian, M. Fatigue improvement of aluminium welds by means of deep rolling and diamond burnishing. *Weld. World* **2022**, *66*, 699–708. [CrossRef]

21. Pavlenko, I.; Simonovskiy, V.; Ivanov, V.; Zajac, J.; Pitel, J. Application of artificial neural network for identification of bearing stiffness characteristics in rotor dynamics analysis. In *Advances in Design, Simulation and Manufacturing, DSMIE 2018*; Ivanov, V., Rong, Y., Trojanowska, J., Venus, J., Liaposhchenko, O., Zajac, J., Pavlenko, I., Edl, M., Perakovic, D., Eds.; Lecture Notes in Mechanical Engineering; Springer: Cham, Switzerland, 2019; pp. 325–335.